On the Stability of Horizontal-to-Vertical Spectrum Ratio of Earthquake Ground Motion

by

Fumio Yamazaki* and Mehedi A. Ansary **

ABSTRACT

Nakamura's method, which uses a horizontal-to-vertical Fourier spectrum ratio of microtremor, has become popular to determine the predominant period and amplification of a site. In this study, this method is extended for earthquake ground motion recordings using new strong motion data recorded by JMA-87-type accelerometers. From the analysis of these accelerograms, horizontal-to-vertical Fourier spectrum ratios of a site for different earthquakes are also found to be stable irrespective of magnitude, distance and depth. To establish this fact, attenuation relations of velocity response spectra for horizontal and vertical components are derived for three damping ratios (0%, 2% and 5%) using the JMA data. Then the horizontal-to-vertical ratios of the velocity response spectra are obtained. The results show that the horizontal and vertical velocity response spectra are dependent on magnitude, distance and depth, but that their ratios are almost independent of magnitude, distance and depth. However, since the current data set consists of mostly intermediate to far field data, this observation should be limited to records of these distance ranges. Introducing station coefficients, representing site amplification, to this relation yields the value comparable to the horizontal-to-vertical Fourier spectrum ratio at a specific site. The stability of the spectrum ratio is explained by the transfer function between the ground surface and stiff-soil outcrop due to S-wave propagation. These results suggest that site amplification characteristics can be evaluated by one-point two-component surface recordings of earthquake ground motion, in a similar manner as proposed by Nakamura for microtremor.

INTRODUCTION

In order to evaluate site amplification characteristics during earthquakes, Nakamura[1] proposed a method to estimate the horizontal-to-vertical (H/V) Fourier spectrum ratio of microtremor. The method was extensively used in Japan[2-4] and in some other countries[5-9].

In the last few years, several researchers[5,7,9] attempted to apply the Nakamura's method (H/V ratio) for earthquake ground motion and compared Fourier spectrum ratios for earthquakes and microtremors. In those studies, applicability of Nakamura's technique for the intense body-wave part of earthquake records were discussed. Then the amplitude ratios were found to be stable irrespective of magnitude, location and depth of earthquake events. However, the physical reason for the stability was not provided by these studies and hence, questions still remain to the applicability of Nakamura's method to earthquakes. From these points of view, this paper attempts to explain the stability of the H/V ratio of Fourier spectra using attenuation relations for earthquake ground motion.

* Institute of Industrial Science, The University of Tokyo, Tokyo, Japan.

** Department of Civil Engineering, BUET, Dhaka 1000, Bangladesh.

There exist a few attenuation models which deal with Fourier spectrum[10,11] and relative velocity response spectrum[12-15]. Theoretically, the Fourier amplitude spectrum can be approximated by the relative velocity response spectrum with low damping ratio. The same form of attenuation models was used for the both types of spectrum amplitudes[14]. Although Trifunac and Lee's attenuation relation[11] considers a local soil type, local geological conditions (depth of sediments) and directional dependence of amplification, these factors are still inadequate to evaluate the local site amplification reliably. More recently, Bozorgnia et al.[13,15] estimated attenuation models of relative velocity spectra for specific fault areas and particular soil types. Also in this paper, attenuation relations for velocity response spectra are used since they have less fluctuation than Fourier spectra do.

As an attenuation model, the one proposed recently by Molas and Yamazaki[16,17] using new JMA (Japan Meteorological Agency) data is selected. The model was proposed for acceleration and velocity response spectra[17] as well as for peak ground acceleration and velocity[16]. In the model, site amplification was considered by assigning a station coefficient for each recording station. This was made possible since several earthquakes were recorded at each JMA station.

In this paper, stability of Fourier spectrum ratio (H/V) for different earthquakes is examined using the JMA records. The stability of the spectrum ratio is reconfirmed through the attenuation relations for the velocity response spectra with low damping ratio. Finally, the reason for the stability of the spectrum ratio is discussed using strong motion data from sites whose soil structures are known and the theoretical transfer functions for S- and P-waves. The aim of this study is to provide a theoretical basis of the use of two-component surface recording at a site for site characterization.

EARTHQUAKE RECORDS

The acceleration records[16] used in this study consist of 2,166 three-component sets from 387 events. These data were recorded by new JMA-87-type accelerometers at 76 free field sites from August 1, 1988 to December 31, 1993. The data set includes records for some major events, such as the Kushiro-Oki Earthquake (M=7.8 in JMA scale) on January 15, 1993, and the Hokkaido-Nansei-Oki Earthquake (M=7.8) on July 12, 1993. Figure 1 shows the locations of the JMA stations and the epicenters of earthquakes used in this study. Records with peak ground accelerations (PGA) less than 1.0 cm/s^2 in one horizontal component were omitted. Events whose focal depths were zero or greater than 200 km were also excluded from the analysis. Figure 2 and Table I show the characteristics of the 387 events and 2,166 data. The records are mostly far-field ones since the records from the 1995 Hyogoken-Nanbu (Kobe) Earthquake are not included in the data set. Information regarding the JMA stations, such as location, soil type, and number of records for each station, is listed in Molas and Yamazaki[16].

The velocity response spectrum, $Sv(\zeta, T)$, used in this study is defined as the maximum response of a ζ (=0, 2 and 5) percent damped single-degree-of-freedom oscillator of varying structural period, T. The responses are calculated by the Newmark's direct integration method from the acceleration time histories. The velocity response spectra for the two horizontal components are calculated and larger of the two in each period, $Sv^H(\zeta, T)$, is used in statistical analysis. The vertical velocity response spectrum, $Sv^V(\zeta, T)$, is also calculated. Twenty two structural periods from 0.05s to 15s (Table I) are selected and a regression analysis is performed separately for each structural period. By treating the attenuation of each structural period as independent to the others, a form of the spectral shape is not imposed.

Table I. Summary of JMA data used in this study

No.of events	387
No. of records	2,166
No. of recording stations	76
Date recorded	August 1, 1988 to December 31, 1993
Instrument	JMA-87 type accelerometers
Recording Institution	Japan Meteorological Agency (JMA)
Magnitude range	4.0 to 7.8 (JMA scale)
Minimum acceleration (for both horizontal components)	PGA≥1.0 gal
Depth range	0.1 km to 200 km
Structural periods analyzed	0.05, 0.06, 0.075, 0.10, 0.12, 0.15, 0.17, 0.20, 0.25, 0.30, 0.40, 0.50, 0.75, 1.0, 1.5, 2.0, 3.0, 4.0, 5.0, 7.5, 10.0, 15.0
Damping ratio	0, 2 and 5 percent of critical

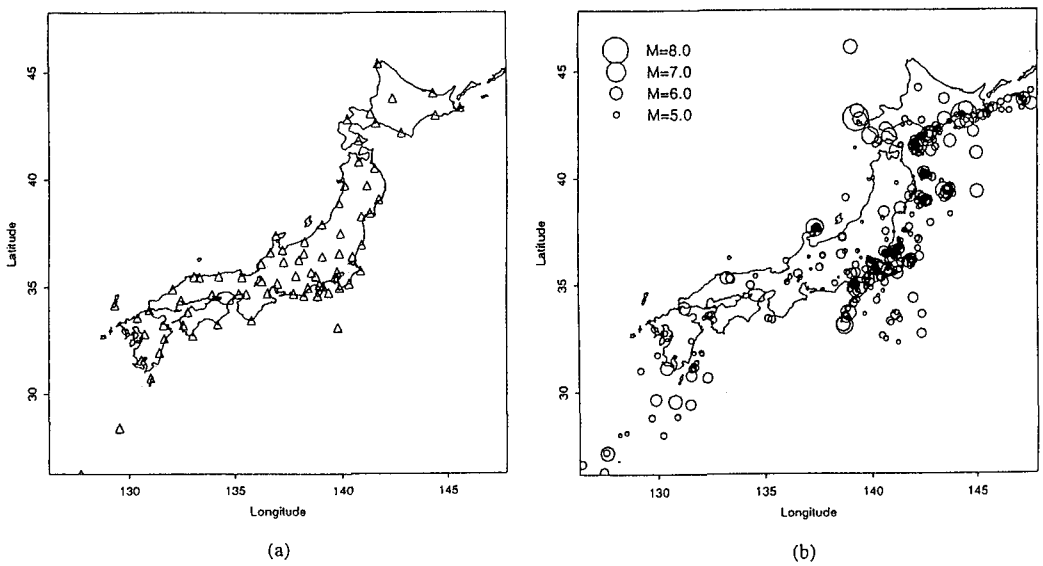

Figure 1. Location of (a) JMA recording stations (triangles) and (b) epicenters of earthquakes (circles) used in this study (Molas and Yamazaki[16])

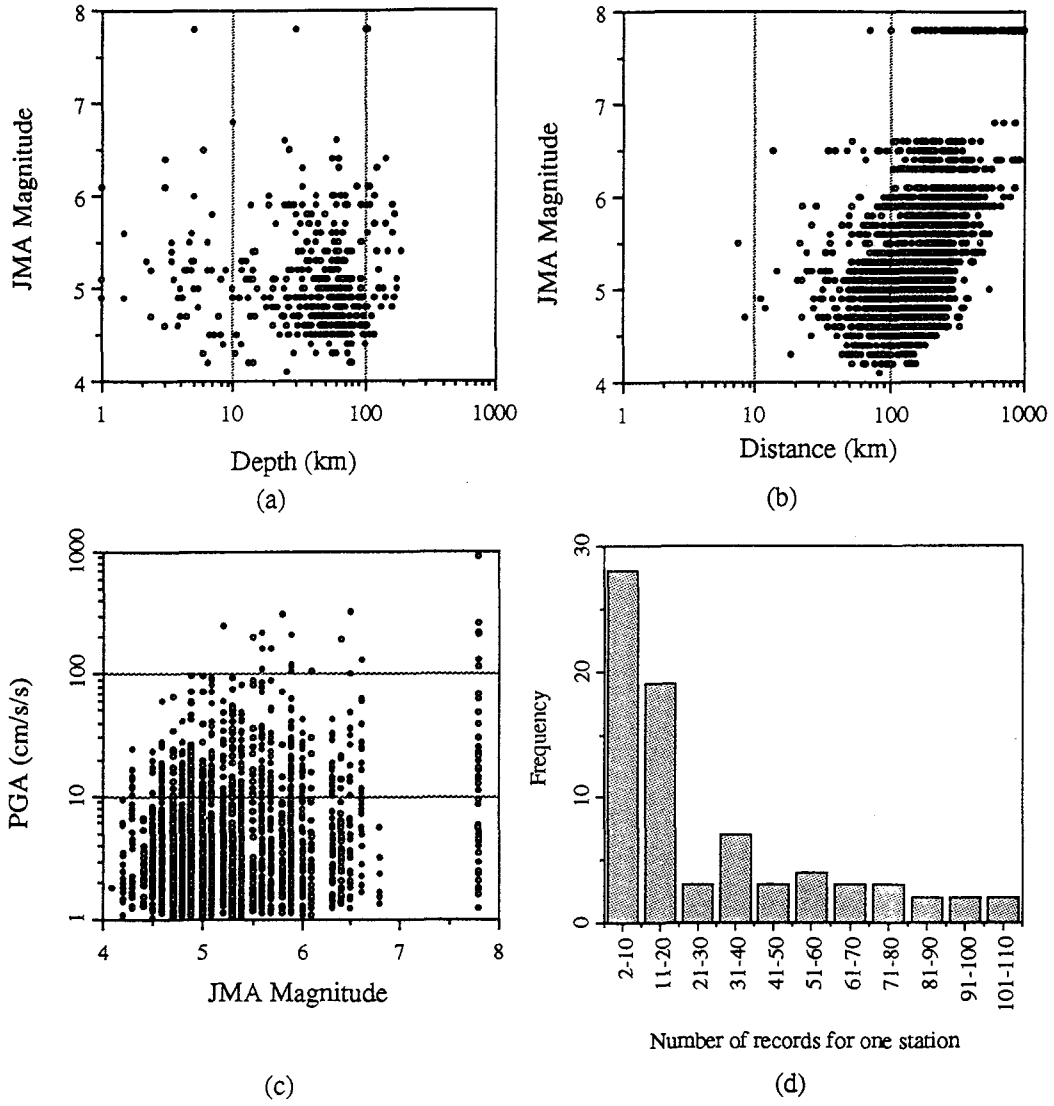

Figure 2. Distribution of (a) depth, (b) distance, and (c) magnitude and peak ground acceleration of the records used in this study and (d) the histogram of the number of records per station (Molas and Yamazaki[16])

STABILITY OF FOURIER SPECTRUM RATIO

The Fourier amplitude ratios of the two horizontal directions of an earthquake record, $R_{NS}(T)$ and $R_{EW}(T)$, are estimated using the following equation:

$$R_{NS}(T) = \frac{F_{NS}(T)}{F_{UD}(T)} \; ; \quad R_{EW}(T) = \frac{F_{EW}(T)}{F_{UD}(T)} \tag{1}$$

where $F_{NS}(T)$, $F_{EW}(T)$ and $F_{UD}(T)$ are the acceleration Fourier amplitude spectra in the NS-, EW- and UD-directions, respectively.

Among the 76 JMA stations, four stations (Hachinohe, Kushiro, Mito, Tokyo) are selected for demonstration of the Fourier spectrum ratios. These stations have observed the largest number of recordings. For each station, ten largest accelerograms were selected for the estimation of the (H/V) Fourier spectrum ratio.

Figure 3 shows the Fourier spectra of the NS- and UD-components for the four JMA stations. Each earthquake record used for this study is at least of 20 s length. Although the amplitude of the Fourier spectra for the different events differ, the shapes of the spectra at the same station show similarity. Figure 3 also shows the Fourier amplitude ratios (H/V) for the two horizontal components. Although the Fourier spectra for different events show wide variability in their amplitudes and some variability in their shapes, the ratios (H/V) of the horizontal and vertical spectral components at a site fall in a narrow range of amplitude and shape. In fact, the Fourier spectrum ratios of earthquake ground motion seem to represent site characteristics; they are stable for different events and show clear peaks. No clear difference is seen for the two horizontal components. The discussion related to the stability of the H/V ratio of the Fourier spectra is provided later.

ATTENUATION MODEL

The attenuation of response spectrum is modeled using the attenuation model proposed by Molas and Yamazaki[16] for the peak ground acceleration and velocity. The model considers the attenuation of seismic waves in a continuous medium with a geometric spreading term, an elastic attenuation term, a depth term and a site-effect term as follows:

$$\log y(T) = b_0(T) + b_1(T)M + b_2(T)r + b_3(T)\log r + b_4(T)h + \sum_{i=1}^{N} c_i(T)S_i + \sigma(T)P \tag{2}$$

where $y(T)$ is the relative velocity response spectrum in cm/s at period T, M is the JMA magnitude, r is the shortest distance in kilometer between the source and the recording station, h is the depth in kilometer of the point on the fault plane that is closest to the recording site, $b_i(T)$'s are the coefficients to be determined for each T and $\sigma(T)$ is the standard deviation of $\log y(T)$ with P=0 for 50-percentiles and P=1 for 84-percentiles. The term $b_2(T)r$ represents anelastic attenuation and the term $b_3(T)\log r$ represents geometric spreading. The geometric spreading constant b_3 is assumed to be -1, which corresponds to a spherical spreading from a point source, since case studies gave inadmissible ranges for b_2 or b_3 if both of them were set free[16]. $c_i(T)$'s are the station coefficients representing local site effect at the recording sites and S_i = 1 for station i, S_i = 0 otherwise. Note that c_i's are constrained to have a zero mean for each period, representing a relative site effect to the average site. N is the total number of recording stations. The total variance σ^2 is taken as $\sigma^2=\sigma_r^2+\sigma_e^2$, where σ_r^2 is the record-to-record (intra-event)

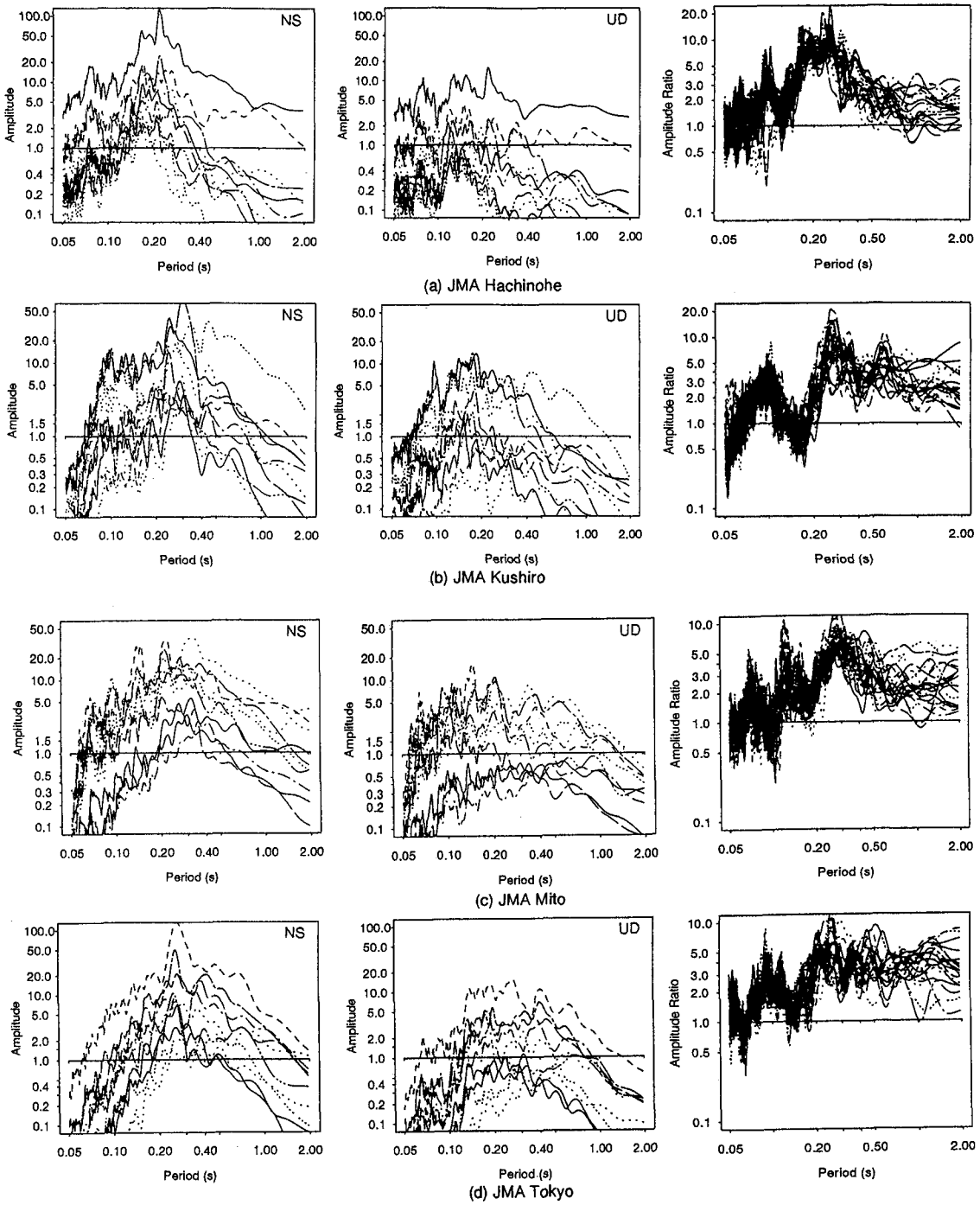

Figure 3. Horizontal (NS) and vertical Fourier spectra, and H/V Fourier spectrum ratio (NS and EW components) of earthquake events at four JMA stations

component of the variance and σ_e^2 is the earthquake-to-earthquake (inter-event) component of the variance. Although the results are not reported here, a preliminary analysis was performed to verify the significance of the depth term and station coefficient to the regression[17].

Although r is defined as the shortest distance from the recording site to the plane of the fault rupture, published reports of fault extent are either difficult to find or nonexistent for the events in the data set except for two large earthquakes (the 1993 Kushiro-Oki and the 1993 Hokkaido-Nansei-Oki with both M=7.8). Because most of the records are in the far-field and smaller magnitude, the use of the hypocentral distance is practical and justified for them.

Since regression analysis is performed for each structural period independently, the index T indicating the frequency dependence of each variable will be dropped from the equations for simplicity. It is thus understood that the regression procedure is performed separately for each structural period.

The attenuation relations of the relative velocity response spectrum with damping ratio ζ, $S_V(\zeta, T)$, for horizontal and vertical components are used to explain the reason behind the stability of the horizontal-to-vertical Fourier spectrum ratio at each station. The attenuation relations for the two components at station i are written as follows for the 50 percentile values:

$$\log S_V^{H}(\zeta,T) = b_0^{H} + b_1^{H} M + b_2^{H} r + b_3^{H} \log r + b_4^{H} h + c_i^{H} \tag{3}$$

$$\log S_V^{V}(\zeta,T) = b_0^{V} + b_1^{V} M + b_2^{V} r + b_3^{V} \log r + b_4^{V} h + c_i^{V} \tag{4}$$

where the superscript "H" represents the horizontal component and "V" the vertical component.

Then the ratio of the two equations yields

$$\log \frac{S_V^{H}(\zeta,T)}{S_V^{V}(\zeta,T)} = (b_0^{H} - b_0^{V}) + (b_1^{H} - b_1^{V}) M + (b_2^{H} - b_2^{V}) r + (b_4^{H} - b_4^{V}) h + (c_i^{H} - c_i^{V}) \tag{5}$$

Note that log r term is dropped in equation (5) due to the assumption of $b_3^{H} = b_3^{V} = -1$. In the following section, variability of $S_V^{H}(\zeta, T)$, $S_V^{V}(\zeta, T)$ and $S_V^{H}(\zeta, T)/S_V^{V}(\zeta, T)$ will be examined as a function of magnitude, distance, depth, and recording site.

ANALYSIS OF HORIZONTAL AND VERTICAL VELOCITY RESPONSE SPECTRA

Regression coefficients

Regression analysis is performed for the relative velocity response spectra with three damping ratios (0%, 2%, 5%) using the JMA data with 2,166 three-component sets. Figure 4 shows the period-dependency of the four regression coefficients (b_0, b_1, b_2, b_4) of the horizontal and vertical velocity response spectra with the three damping ratios. The coefficients for three damping ratios looks quite similar for both horizontal and vertical components. Note that the approximation of acceleration Fourier spectrum by velocity response spectrum is valid for zero damping ratio. But at zero damping, the response spectrum may fluctuate. Since the regression coefficients are close for the three damping ratios, a small damping value (2%) is used in the following analysis. Tables II and III show the regression coefficients of the relative velocity response spectra with 2% damping for the horizontal and vertical components, respectively.

In Figure 4, the four regression coefficients for the horizontal and vertical components are seen to behave quite similar manner to the period axis. The regression intercept, b_0, for the horizontal component is slightly higher than that for the vertical component although their trends are very similar. The magnitude coefficient, b_1, is almost the same for the two components. The

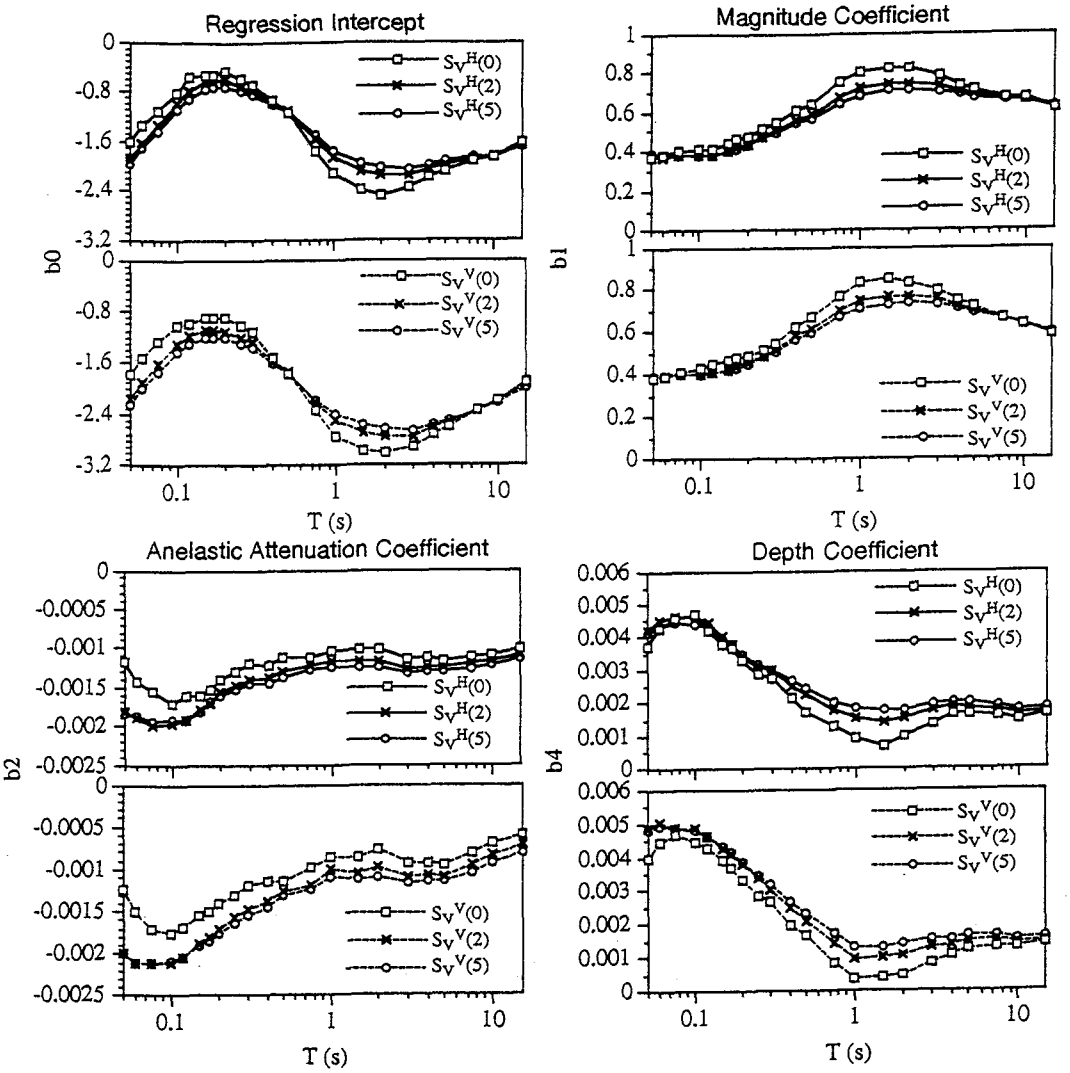

Figure 4. Regression coefficients for attenuation relations of $S_V^H(\zeta, T)$ and $S_V^V(\zeta, T)$ for three damping ratios (0%, 2% and 5%)

Table II. Regression coefficients for relative velocity response spectrum, $S_V^H(0.02, T)$, for horizontal component (in cm/s)

T (sec)	b_0	b_1	b_2	b_3	b_4	σ_r	σ_e	σ
0.05	-1.8997	0.3792	-0.00182	-1.00	0.00424	0.268	0.179	0.322
0.06	-1.6373	0.3752	-0.00189	-1.00	0.00449	0.274	0.177	0.326
0.075	-1.3705	0.3832	-0.00199	-1.00	0.00461	0.278	0.192	0.338
0.10	-0.9802	0.3784	-0.00197	-1.00	0.00465	0.277	0.193	0.337
0.12	-0.7882	0.3843	-0.00192	-1.00	0.00445	0.273	0.192	0.334
0.15	-0.6324	0.4006	-0.00180	-1.00	0.00400	0.274	0.183	0.330
0.17	-0.6410	0.4211	-0.00172	-1.00	0.00381	0.273	0.161	0.317
0.20	-0.6077	0.4358	-0.00156	-1.00	0.00344	0.274	0.148	0.311
0.25	-0.7203	0.4780	-0.00149	-1.00	0.00313	0.263	0.142	0.299
0.30	-0.7862	0.5038	-0.00141	-1.00	0.00297	0.259	0.132	0.291
0.40	-0.9935	0.5571	-0.00139	-1.00	0.00252	0.246	0.132	0.279
0.50	-1.1358	0.5868	-0.00130	-1.00	0.00225	0.239	0.118	0.266
0.75	-1.5870	0.6712	-0.00123	-1.00	0.00180	0.232	0.120	0.261
1.00	-1.8828	0.7156	-0.00117	-1.00	0.00153	0.228	0.113	0.254
1.50	-2.1044	0.7403	-0.00116	-1.00	0.00143	0.225	0.107	0.249
2.00	-2.1734	0.7407	-0.00117	-1.00	0.00153	0.228	0.105	0.250
3.00	-2.1650	0.7269	-0.00127	-1.00	0.00178	0.232	0.104	0.254
4.00	-2.0672	0.7003	-0.00125	-1.00	0.00191	0.233	0.100	0.253
5.00	-2.0003	0.6848	-0.00125	-1.00	0.00187	0.235	0.101	0.256
7.50	-1.9082	0.6633	-0.00121	-1.00	0.00180	0.240	0.102	0.261
10.00	-1.8767	0.6600	-0.00118	-1.00	0.00166	0.238	0.114	0.264
15.00	-1.6863	0.6211	-0.00109	-1.00	0.00175	0.236	0.104	0.258

σ_r^2 = record to record component of variance (determined in second step)

σ_e^2 = earthquake to earthquake component of variance (determined in third step)

σ^2 = total variance $\equiv \sigma_r^2 + \sigma_e^2$

Table III. Regression coefficients for relative velocity response spectrum, $S_V^V(0.02, T)$, for vertical component (in cm/s)

T (sec)	b_0	b_1	b_2	b_3	b_4	σ_r	σ_e	σ
0.05	-2.1394	0.3892	-0.00200	-1.00	0.00490	0.256	0.186	0.317
0.06	-1.9100	0.3966	-0.00211	-1.00	0.00502	0.264	0.191	0.326
0.075	-1.6104	0.4010	-0.00211	-1.00	0.00489	0.261	0.200	0.329
0.10	-1.3084	0.4070	-0.00210	-1.00	0.00487	0.257	0.199	0.325
0.12	-1.1888	0.4162	-0.00203	-1.00	0.00462	0.249	0.187	0.321
0.15	-1.0766	0.4275	-0.00187	-1.00	0.00428	0.246	0.174	0.301
0.17	-1.0868	0.4424	-0.00181	-1.00	0.00411	0.245	0.162	0.307
0.20	-1.0981	0.4584	-0.00171	-1.00	0.00378	0.247	0.148	0.288
0.25	-1.1974	0.4914	-0.00156	-1.00	0.00337	0.235	0.135	0.271
0.30	-1.2719	0.5159	-0.00147	-1.00	0.00304	0.233	0.123	0.264
0.40	-1.5820	0.5819	-0.00139	-1.00	0.00247	0.220	0.128	0.255
0.50	-1.7502	0.6129	-0.00127	-1.00	0.00210	0.209	0.129	0.246
0.75	-2.2143	0.7013	-0.00119	-1.00	0.00142	0.205	0.130	0.243
1.00	-2.4864	0.7458	-0.00100	-1.00	0.00094	0.198	0.125	0.234
1.50	-2.6769	0.7663	-0.00105	-1.00	0.00100	0.191	0.118	0.224
2.00	-2.7361	0.7640	-0.00097	-1.00	0.00107	0.193	0.107	0.221
3.00	-2.7390	0.7549	-0.00109	-1.00	0.00128	0.198	0.112	0.227
4.00	-2.6007	0.7202	-0.00107	-1.00	0.00137	0.196	0.116	0.228
5.00	-2.5317	0.7037	-0.00110	-1.00	0.00149	0.201	0.113	0.231
7.50	-2.3368	0.6609	-0.00096	-1.00	0.00153	0.202	0.117	0.234
10.00	-2.1932	0.6336	-0.00084	-1.00	0.00145	0.202	0.120	0.235
15.00	-1.9450	0.5857	-0.00072	-1.00	0.00150	0.204	0.114	0.234

coefficient is nearly constant at periods below 0.1s, it has an increasing trend as the structural period increases from 0.1s to 1.5s and has an decreasing trend as the structural period increases from 1.5s to 15s. Similar trends have also been observed by Joyner and Boore[12].

The absolute value of the anelastic attenuation rate, b_2, decreases as the structural period increase. This trend is consistent with the observation that high-frequency contents of strong ground motion are attenuated faster than low-frequency contents. The depth effect coefficient, b_4, decreases as the structural period increases. The depth effect becomes almost constant for periods of 1s and above.

Spectral shape

An important aspect of response spectra is the spectral shape since this will largely determine the expected response of a given structure. By taking the regression for several structural periods independently, it is not necessary to pre-determine the shape of response spectra. Figure 5 compares the spectral shapes for different magnitudes, source-site distances, and source depth. Note that the station coefficient is set to be the mean value (c_i =0) of all the stations in the figure. It can be seen that the spectral amplitude of both the horizontal and vertical velocity responses depend on magnitude and distance, and to some extent on depth.

Figures 5a and 5b show the mean horizontal and vertical velocity response spectra (S_V) for a given depth and distance with changes in magnitude. The structural period where the peak of the response spectra occurs increases as the magnitude increases. Figures 5d and 5e compare the mean horizontal and vertical S_V for a given magnitude and depth with changes in the shortest distance. Figures 5g and 5h show the mean horizontal and vertical S_V for a given magnitude and source-site distance with changes in depth. Higher response can be observed for deeper events. There is a slight shift of the peak to a shorter structural period as the source depth increases, particularly for the vertical component.

Spectrum ratio

Horizontal-to-vertical velocity response spectral ratios were calculated for different magnitudes, source-site distances, and source depths. Figure 5c shows the velocity response spectral ratio for a given depth and shortest distance with changes in magnitude. The ratio is slightly affected by the magnitude, but the overall shape is similar. In the very short-period range (less than 0.1s), the ratio is almost constant (about 1.5); in the short-period range (0.1s to 0.5s), the ratio increases linearly with period (up to 2.7-3.2); in the intermediate to long-period range (0.5s to 7.5s), the ratio becomes almost constant. In these period ranges, the ratio is larger for smaller magnitude events but for the long-period range (greater than 7.5s), the ratio becomes larger for larger magnitude events. The trend of the spectrum ratio is consistent with the fact that the vertical component has higher frequency contents than those of the horizontal components. Similar observations were found in previous studies[13].

Figure 5f shows the response spectrum ratio for a given magnitude and depth with changes in distance. The trend of variation of the ratio with period is same as Figure 5c. The effect of variation of distance is almost negligible. However, this may not be true for near-field recordings, e.g., those in the 1995 Hyogoken-Nanbu (Kobe) Earthquake. Since the current data set consists of mostly intermediate to far field data (Figure 2), this observation should be limited to records of these distance ranges. For near-field recordings, further research on H/V spectrum ratio is necessary. It is also better to be mentioned that the H/V spectrum ratio may change if the amplitude of ground motion reaches the level to cause soil non-linearity; the horizontal component is affected by reduction of shear rigidity and increase of damping ratio while the vertical component is scarcely affected. The extreme case is the occurrence of liquefaction, in which

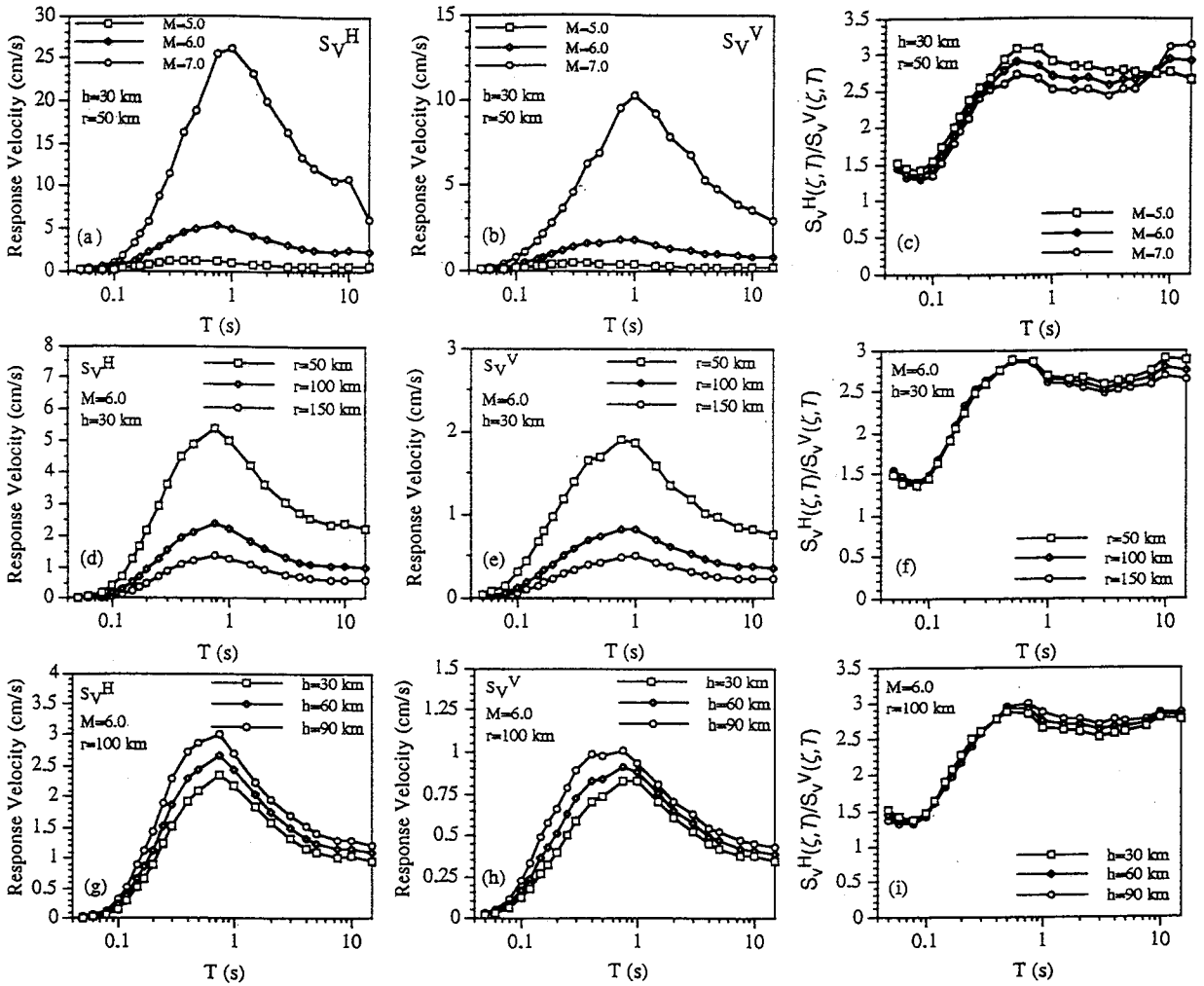

Figure 5. Predicted horizontal and vertical velocity response spectra, and horizontal-to-vertical (H/V) velocity response spectrum ratio for 2% damping and c_i=0.0

horizontal motion is de-amplified while vertical motion is not so much affected, as seen in the vertical array records of Kobe Port Island[18].

Figure 5i shows the spectrum ratio for a given magnitude and distance with changes in depth. The variation of the ratio with different depth is again very small.

In summary, the ratio of horizontal-to-vertical velocity response spectra (H/V) of intermediate to far field records is a function of period, but almost independent of magnitude, source-site distance and source depth. Hence, in equation (5), only b_0 term remains if the site effect is not considered.

Site-specific response spectrum ratio

Figure 6 shows the station coefficient spectrum[17] for the four stations. The shapes are different from station to station. But, for the same site, the station coefficient spectrum for the vertical component has the similar shape with that for the horizontal component. It is also seen from the figure that the period corresponding to the peak for the vertical component is shorter than that for the horizontal one. Molas and Yamazaki[17] inferred that the peak of the station coefficient spectrum for the horizontal response spectrum corresponds to the predominant period of S-wave propagation. As an extension of this inference, the peak for the vertical component may indicate the predominant period of P-wave propagation. However, it is difficult to prove this for the JMA stations since detailed geological profiles are not available.

By combining the velocity response spectrum ratio for the mean station (with c_i=0.0) and the spectrum of station coefficients (c_i^H and c_i^V), the site-specific response spectrum ratio can be obtained for each JMA station. Figure 7 shows sample site-specific velocity response spectrum ratios for the four JMA stations plotted for a particular distance, depth and magnitudes. The site-specific response spectrum ratios show clear peaks and the effect of magnitude on the ratios seems almost negligible. Since the effects of distance and depth have already been shown to be small (see Figure 5) for the current data set, the spectrum ratio is unique to the site. Thus the H/V response spectrum ratio R_i at a specific site i is approximated as a function of structural period only as

$$\log R_i = \log \frac{S_V^H(\zeta,T)}{S_V^V(\zeta,T)} \approx \left[b_0^H(T) - b_0^V(T)\right] + \left[c_i^H(T) - c_i^V(T)\right] \qquad (6)$$

where the first term of the right side of equation (6) shows the spectrum ratio on the average site (see Figures 5c, 5f, 5i) and the second term represents the site effect (see Figure 6).

Fourier spectrum ratio vs. response spectrum ratio

In Figure 8, the response spectrum ratio for 2% damping (Figure 7) is compared with the Fourier spectrum ratio (Figure 3) for the four JMA sites. Although slight dependence of the response spectrum ratio on magnitude, depth and distance exists, it may be insignificant for this comparison. In the figure, the mean Fourier spectrum ratio is shown together with the mean plus or minus one standard deviation. As expected, the comparison reveals that the predicted velocity response spectral ratio at low damping ratio produces similar values with the average of the observed Fourier spectrum ratio. Hence, the stability of H/V ratio of Fourier spectra at each site is reconfirmed using the attenuation relations for S_V and the approximation between Fourier spectrum and S_V.

Proximity of the spectrum ratio and transfer function

Uniqueness of horizontal-to-vertical spectrum ratio (H/V) at each site was shown above. However, the implication of the H/V ratio has not been explained. To perform this task, earthquake records from two downhole array sites in the Tokyo metropolitan area are employed.

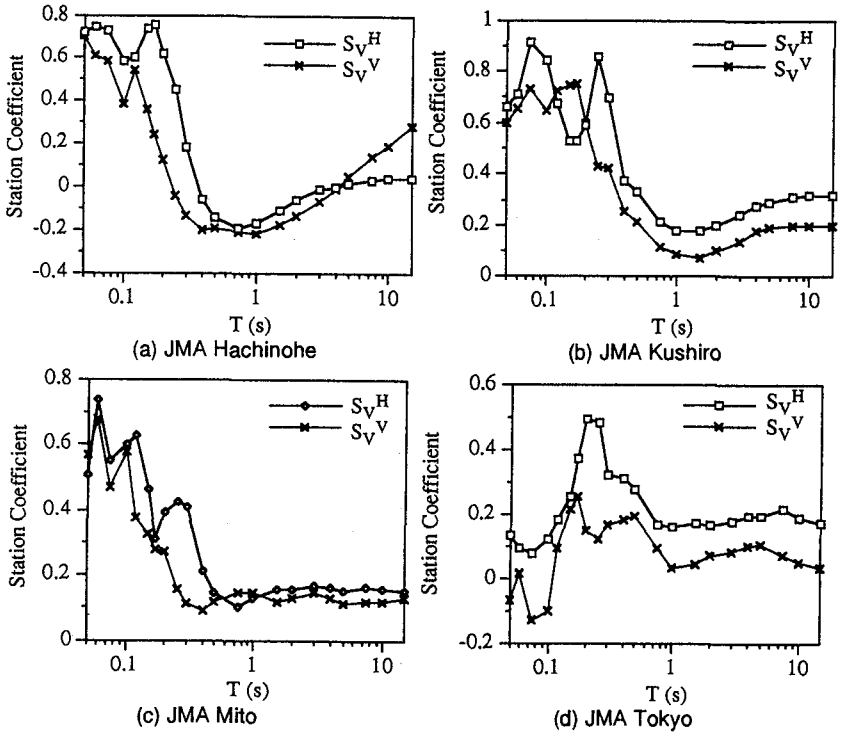

Figure 6. Comparison of station coefficients for attenuation relations of $S_V^H(0.02, T)$ and $S_V^V(0.02, T)$ for four JMA stations

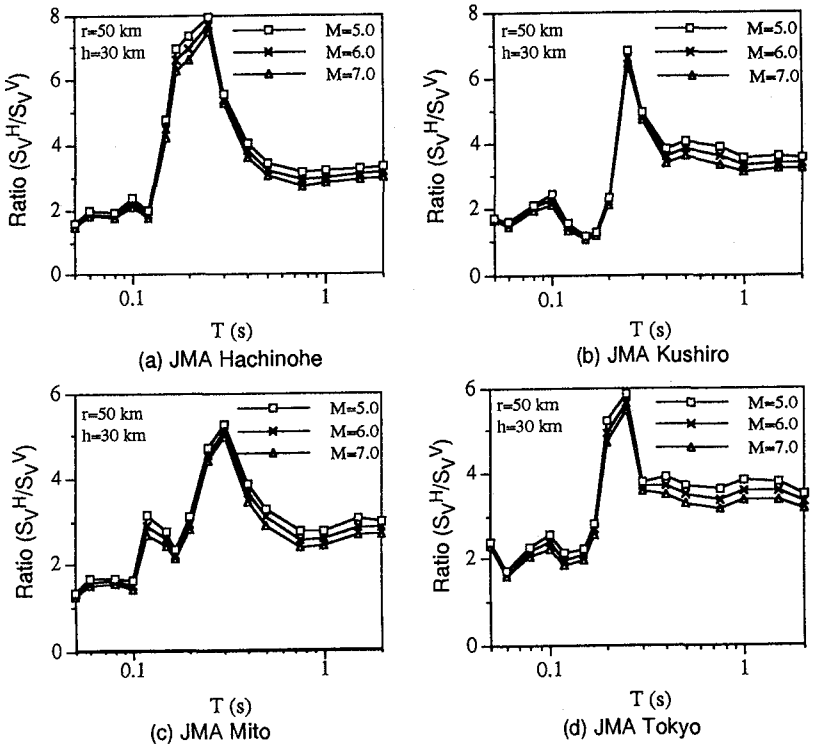

Figure 7. Predicted horizontal-to-vertical (H/V) velocity response spectrum ratio with 2% damping for four JMA stations

At these sites (Soka and Kodaira), underground structures were surveyed by PS-logging (Tables IV and V). In addition, microtremor observation was recently conducted by the present authors[4].

Figure 9 shows the theoretical transfer functions for one-dimensional S-wave and P-wave propagation using the wave velocities measured by the PS-logging. As shown in the schematic drawing in Figure 9, the transfer function represents the spectrum ratio between the free surface motion ($2E_s$) and the base (at the bottom of soil columns in Tables IV and V) outcrop motion ($2E_r$) for the horizontal or vertical component. In the figure, the ratio $r_T = A_H/A_V$ of the horizontal transfer function A_H ($=E_s^H/E_r^H$) and the vertical transfer function A_V ($=E_s^V/E_r^V$) is also plotted. It is seen that, for Soka, the transfer function ratio is almost same as the horizontal transfer function because the vertical transfer function is almost constant in the range (0.05s to 2.0s). The transfer function ratio for Kodaira is also close to the horizontal transfer function, but its second peak is suppressed because it is close to the first peak of the vertical transfer function. From these plots, the approximation of the horizontal (S-wave) transfer function by the H/V transfer function ratio seems to be valid near the first natural frequency of S-wave propagation for ordinary soil conditions.

Although the dominant peak of the H/V ratio may be determined by the site-specific term ($c_i^H - c_i^V$) for most cases, the non-site-specific term ($b0^H - b0^V$) also affects the H/V ratio of response spectra (thus Fourier spectra). This fact is examined by the examples of Soka and Kodaira. For these sites, S and P-wave velocities are known, but station coefficients are unknown. Using the following relationship

$$r_T = \frac{A_H}{A_V} = \frac{E_s^H/E_r^H}{E_s^V/E_r^V} = \frac{(E_s^H/E_s^V)}{(E_r^H/E_r^V)} \approx \frac{R_{surface}}{R_{reference}} \tag{7}$$

the H/V response spectrum ratio $R_{surface}$ at the surface of a site is approximated by

$$R_{surface} \approx r_T R_{reference} \tag{8}$$

where r_T is the transfer function ratio and $R_{reference}$ is the H/V response spectrum ratio for the base outcrop motion. Note that the "reference" point of the transfer function is also outcrop (surface) and its H/V spectrum ratio is free from the site effect if the soil column is modeled to the depth of stiff-soil layers. Considering equation (6), it may be reasonable to assume $R_{reference} = 10^{**}(b0^H - b0^V)$. However, note that $b0^H$ and $b0^V$ are determined in a manner that the average station coefficient for the JMA sites becomes zero ($c_i^H = c_i^V = 0$) and thus the reference points of the transfer function for Soka and Kodaira seem to be stiffer than the average ground of the JMA stations.

Figure 10 compares the response spectrum ratio $R_{surface}$ (dots) estimated by equation (8) and the average of Fourier spectrum ratios (thin solid line) for seven small-amplitude earthquake records for Soka and Kodaira. Although some difference is observed for their amplitudes, their trends are quite similar. The first mode peak for S-wave is clearly seen for both ratios. Except for the peak at about 0.2 s for the Fourier spectrum ratio at Kodaira, good agreement is seen in the shapes of ratios for the both sites. The difference in amplitude can be explained by the difference of the reference points mentioned above (the estimated $R_{surface}$ looks larger than the observed H/V ratio since $R_{reference}$ may be overestimated).

Due to the similarity of the transfer function ratio and the S-wave transfer function ($r_T \approx A_H$, see Figure 9), the Fourier spectrum ratio can also estimated by $R_{surface} \approx A_H * 10^{**}(b0^H - b0^V)$ in the period range around the first predominant period of S-wave propagation. Since the term $10^{**}(b0^H - b0^V)$ is almost constant in a wide period range (0.5 s- 7.5 s, see Figure 5), the first predominant period of S-wave transfer function (A_H, thick solid line) coincides with that of

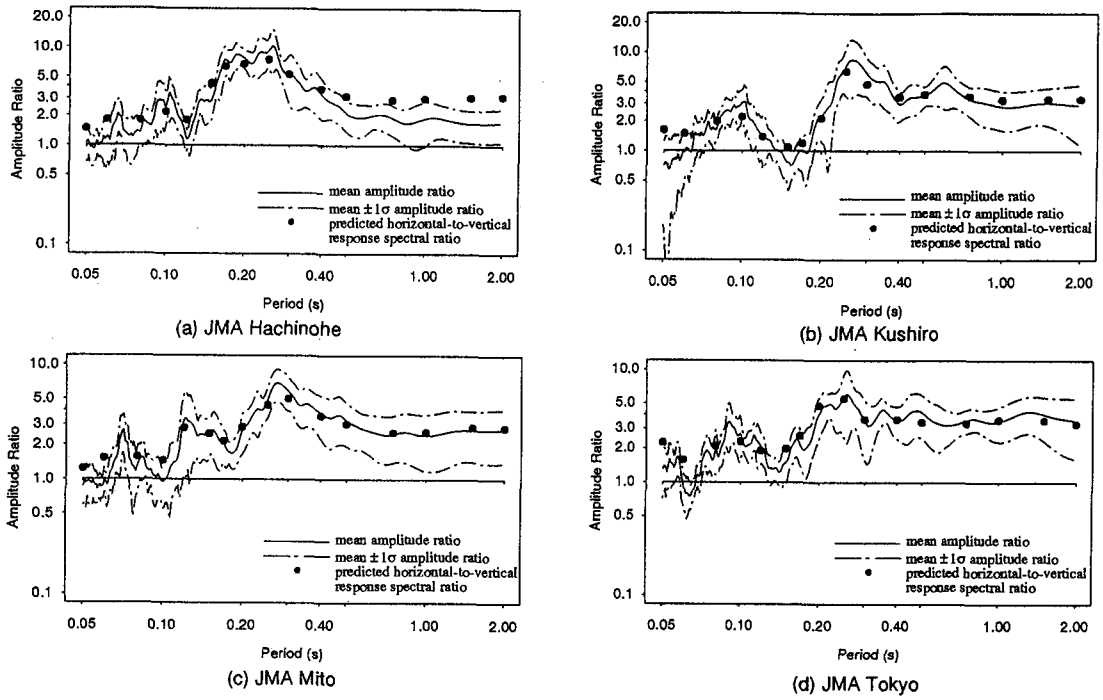

Figure 8. Comparison between predicted horizontal-to-vertical velocity response spectrum ratio at 2% damping (symbols), mean observed Fourier amplitude ratio (solid line) and mean plus or minus one standard deviation (dashed lines) for four JMA stations

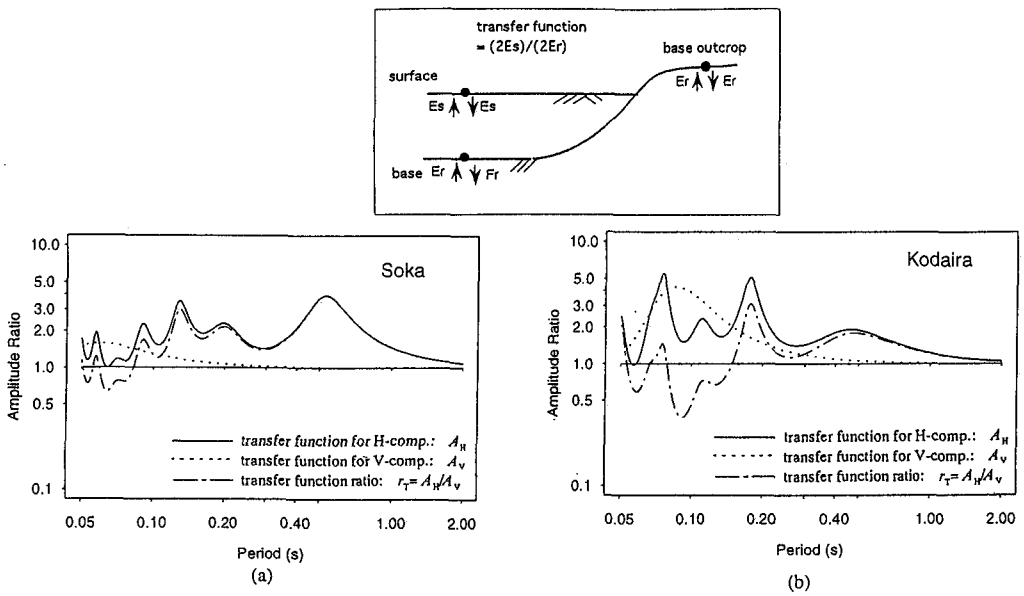

Figure 9. Comparison of transfer functions for horizontal (A_H) and vertical (A_V) components and their ratio (r_T) at (a) Soka and (b) Kodaira downhole arrays

Table IV. Soil profile of Soka site

Layer Thickness m	Density t/m^3	P-wave Velocity m/s	S-wave Velocity m/s	Poisson's Ratio
1.50	1.50	300	100	0.438
2.10	1.50	1510	100	0.498
2.35	1.70	1510	140	0.496
5.75	1.60	1510	110	0.497
6.90	1.65	1380	190	0.490
5.15	1.65	1380	260	0.482
5.00	2.10	1950	490	0.466
3.05	1.85	1800	380	0.477
3.70	1.90	1800	480	0.412

Table V. Soil profile of Kodaira site

Layer Thickness m	Density t/m^3	P-wave Velocity m/s	S-wave Velocity m/s	Poisson's Ratio
1.50	1.50	290	80	0.46
6.70	1.60	390	180	0.37
4.80	2.00	950	500	0.31
3.70	2.00	1710	500	0.45
5.10	1.85	1710	420	0.47
2.00	1.85	1710	370	0.48
3.70	2.00	1710	430	0.47
5.20	1.80	1500	340	0.47
8.30	1.80	1500	320	0.48
5.50	2.00	2040	620	0.45

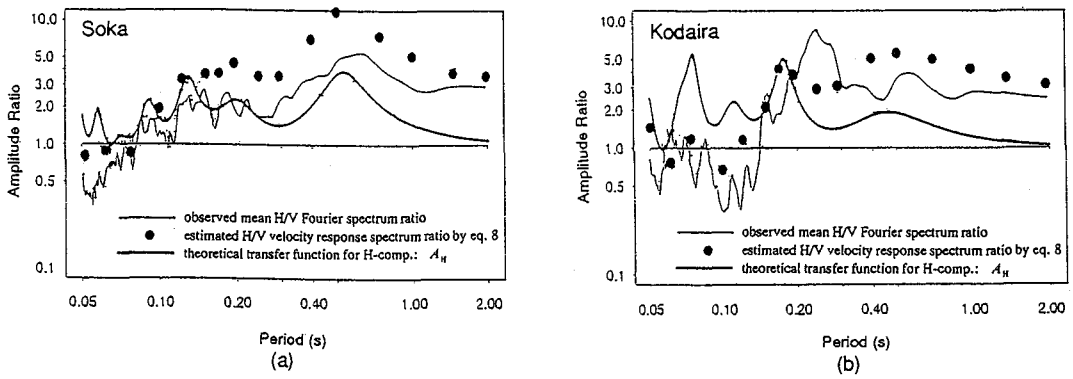

Figure 10. Comparison between observed H/V Fourier spectrum ratio (thin line), estimated H/V velocity response spectrum ratio by equation 8 (dots), and transfer function (A_H) for horizontal component (bold line) for (a) Soka and (b) Kodaira

$R_{surface}$ as shown in Figure 10. Note that this comparison is just for peak periods, not for amplitudes.

These observations suggest the theoretical background of proximity of the H/V ratio of Fourier spectra at the ground surface and the S-wave transfer function between the ground surface and stiff-soil outcrop. Hence the predominant period of a site can be estimated from two-component earthquake records at the surface of the site in approximation.

CONCLUSIONS

The amplitude ratio (H/V) of horizontal and vertical Fourier spectra, defined by Nakamura for microtremor at a site, has been extended to earthquake recordings. At four JMA stations, where triaxial accelerometers are deployed, Fourier spectra were calculated for several earthquake events. Although the amplitudes of both the horizontal and vertical Fourier spectra varied from event to event, their ratios (H/V) were found to be stable for different events at each site.

In order to explore a physical reason for this observation, attenuation relations of relative velocity response spectra for horizontal and vertical components were derived for each structural period using 2,166 recordings by JMA-87-type accelerometers from 76 JMA stations. The attenuation relations were constructed as a function of magnitude, source-site distance, source depth, and station coefficient. As a result of regression analysis, the magnitude, distance, and depth dependent terms were found to be close for the horizontal and vertical components. Hence, if we take the spectrum ratio of the two components, the ratio can be approximated by only a function of station coefficients, which represent site characteristics for the two components. Through the proximity of Fourier spectra and velocity response spectra with small damping, the stability of the Fourier spectrum ratio (H/V) was confirmed. This observation is limited to intermediate to far field records, however, because of the data set used in the analysis.

Implication of the H/V spectrum ratio was further investigated using earthquake records from downhole array sites whose underground structures were known. The transfer functions between the ground surface and outcrop base were calculated for the S-wave and P-wave propagation in the vertical direction. Then the ratio of the transfer functions was also calculated. The result showed that the transfer function ratio is close to the S-wave transfer function around the predominant period of the S-wave. The H/V Fourier spectrum ratio from earthquake records was then compared with the transfer function ratio multiplied by the non-site-specific term of the H/V response spectrum ratio. Good agreement between them shows the validity for the physical insight to the H/V spectrum ratio of earthquake ground motion. The similarity between the site-specific H/V spectrum ratio and the S-wave transfer function was also demonstrated.

These results suggest that site amplification characteristics can be evaluated by one-point two-component surface recordings of earthquake ground motion, in a similar manner as proposed by Nakamura for microtremor.

REFERENCES

1. Y. Nakamura, 'A method for dynamic characteristics estimation of subsurface using microtremor on the ground surface', *QR of RTRI* **30**, 25-33 (1989).
2. T. Ohmachi, T. Shimizu and K. Konno, 'Seismic zoning of Yokohama city based on microtremor measurement at jounior high schools', *Proc. 5th int. conf. on seismic zonation.* **I**, 873-880 (1995).

3. K. Tokimatsu and H. Arai, 'Estimation of local site conditions in Kushiro city based on array observation of microtremors', *Proc. 3rd int. conf. on recent advances in geotechnical earthquake eng. and soil dyn.* **II**, 599-602 (1995).
4. M. A. Ansary, M. Fuse, F. Yamazaki and T. Katayama, 'Use of microtremors for the estimation of ground vibration characteristics', *Proc. 3rd int. conf. on recent advances in geotechnical earthquake eng. and soil dyn.* **II**, 571-574 (1995).
5. J. Lermo and F. J. Chavez-Garcia, 'Site effect evaluation using spectral ratios with only one station', *Bull. seism. soc. Am.* **83**, 1574-1594 (1993).
6. J. Lermo and F. J. Chavez-Garcia, 'Are microtremors useful in site response evaluation', *Bull. seism. soc. Am.* **84**, 1350-1364 (1994).
7. E. H. Field and K. H. Jacob, 'A comparison and test of various site-response estimation techniques, including three that are not reference-site dependent', *Bull. seism. soc. Am.* **85**, 1127-1143 (1995).
8. C. Lachet and P. Y. Bard, 'Theoretical investigations on the Nakamura's technique', *Proc. 3rd int. conf. on recent advances in geotechnical earthquake eng. and soil dyn.* **II**, 671-675 (1995).
9. N. P. Theodulidis and P. Y. Bard, 'Horizontal to vertical spectral ratio and geological conditions: an analysis of strong motion data from Greece and Taiwan (SMART-1)', *Soil dyn. earthquake eng.* **14**, 177-197 (1995).
10. L. Mamula, K. Kudo and E.Shima, 'Distribution of ground-motion amplification factors as a function of period (3-15 sec), in Japan', *Bull. of earthquake research institute* **59**, 467-500 (1984).
11. M. D. Trifunac and V. W. Lee, 'Empirical models for scaling Fourier amplitude spectra of strong ground acceleration in terms of earthquake magnitude source to station distance, site intensity and recording site conditions', *Soil dyn. earthquake eng.* **8**, 110-125 (1989).
12. W. B. Joyner, and D. M. Boore, 'Estimation of response spectral values as functions of magnitude, distance and site conditions', *Open File Report 82-881*, U.S. Geological Survey, 1982.
13. Y. Bozorgnia and M. Niazi, 'Distance scaling of vertical and horizontal response spectra of the Loma Prieta Earthquake', *Earthquake eng. struct. dyn.* **22**, 695-707 (1993).
14. V. W. Lee, 'Scaling PSV from earthquake magnitude, local soil, and geologic depth of sediments', *J. Geotech. Engg., ASCE* **119**, 108-126 (1993).
15. Y. Bozorgnia, M. Niazi and K. W. Campbell, 'Characteristics of free-field vertical ground motion during the Northridge Earthquake', *Earthquake Spectra* **11**, 515-525 (1995).
16. G. L. Molas and F. Yamazaki, 'Attenuation of earthquake ground motion in Japan including deep focus events', *Bull. seism. soc. Am.* **85**, 1343-1358 (1995a).
17. G. L. Molas and F. Yamazaki, 'The effect of source depth and local site to the attenuation characteristics of response spectra', *Proc. 23rd JSCE earthq. eng. sym.*, 69-72 (1995b).
18. Y. Iwasaki and M. Tai, 'Strong motion records at Kobe Port Island', *Special Issue of Soils and Foundations*, Japanese Geotechnical Society, 29-40 (1996).